Evaporation of the Pancake-Vortex Lattice in Weakly Coupled Layered Superconductors

M. J. W. Dodgson,[1,*] A. E. Koshelev,[2] V. B. Geshkenbein,[1,3] and G. Blatter[1]

[1]*Theoretische Physik, ETH-Hönggerberg, CH-8093, Zürich, Switzerland*

[2]*Materials Science Division, Argonne National Laboratory, 9700 South Cass Avenue, Argonne, Illinois 60439*

[3]*L. D. Landau Institute for Theoretical Physics, 117940 Moscow, Russia*

(Received 29 November 1999)

We calculate the melting line of the pancake-vortex system in a layered superconductor, interpolating between two-dimensional (2D) melting at high fields and the zero-field limit of single-stack evaporation. Long-range interactions between pancake vortices in different layers permit a mean-field approach, the "substrate model," where each 2D crystal fluctuates in a substrate potential due to the vortices in other layers. We find the thermal stability limit of the 3D solid, and compare the free energy to a 2D liquid to determine the first-order melting transition and its jump in entropy.

PACS numbers: 74.60.Ge, 74.80.Dm

The pancake-vortex lattice in layered superconductors defines a tunable soft matter system with astonishing properties [1]. Among them, the thermodynamic phase transition of vortex-lattice melting and its first-order character is now experimentally well established [2,3], but questions remain as to which correlations are lost at the transition [4]. Theoretically, the position of the melting line can be estimated with a Lindemann criterion [5,6], but a more detailed description of melting is required to determine the characteristics of the transition. The challenge in defining a theoretical scheme describing vortex-lattice melting follows from the complexity of the vortex system in real superconductors combined with the general lack of exact theories of melting.

In a moderately anisotropic material, such as $YBa_2Cu_3O_7$, the vortex crystal melts to a line liquid and numerical simulations have treated this in detail [7]. In $Bi_2Sr_2CaCu_2O_8$ (BSCCO), however, the coupling between layers is so weak that the layered structure (with spacing d) plays a crucial role, and the vortex matter acts as a collection of interacting two-dimensional (2D) vortices, or pancake vortices. Rather than using numerical simulations [8,9], we describe here a novel analytic treatment to track the melting line through the B-T phase diagram in the extreme anisotropic limit of zero Josephson coupling between layers. In this limit the 3D pancake-vortex lattice (PVL) remains stable at low temperatures due to an attractive electromagnetic interaction between pancake vortices in different layers, with range $\lambda \gg d$ (λ is the in-plane penetration depth). Changing the magnetic field tunes the relative importance of this attractive interlayer interaction and the long-range repulsion between vortices in the same layer. At high fields, $B \gg B_\lambda = \Phi_0/\lambda^2$, the in-plane interactions dominate and the 3D lattice melts to independent 2D liquids (a pancake-vortex gas) close to the 2D melting temperature $T_m^{2D} \approx \varepsilon_0 d/70$ [10] [where $\varepsilon_0 = (\Phi_0/4\pi\lambda)^2$]. At lower fields the interlayer attraction stabilizes the lattice and increases the melting temperature. In the low-field limit of weakly coupled 1D stacks, the crystal melts below the evaporation transition of an isolated stack of pancake vortices [11] located at the Berezinskii-Kosterlitz-Thouless (BKT) vortex unbinding transition [12] of an isolated layer at $T_{\mathrm{BKT}} = \varepsilon_0 d/2 \sim 35 T_m^{2D}$. The field regime $B \sim B_\lambda$ where the melting line interpolates between the above limits then spans a factor $\sim$35 in "reduced" temperature $T/\varepsilon_0 d$ (in real superconductors ε_0 vanishes as T_c is approached, and the real temperature ratio $T_{\mathrm{BKT}}/T_m^{2D}$ will be smaller). Before reaching zero field, the melting line is cut by a competing low-field reentrant transition to a dilute liquid of stacks with exponentially weak interactions [1]. A Lindemann analysis [6] tells us that at $T \sim \varepsilon_0 d/2$ reentrant melting occurs at a field below $10^{-2} B_\lambda$.

Ignoring reentrance, we have a 3D melting line that interpolates between a 1D stack evaporation (exactly described by 2D BKT theory) and a 2D melting transition usually described by a BKT-type mechanism of dislocation pair unbinding. Both limits are well described by a self-consistent approximation and we here generalize this to all magnetic fields. Our self-consistent method relies on the long range of the interlayer attractions; each pancake vortex feels the attractive force of pancake vortices in $\sim\lambda/d$ other layers. Therefore the fluctuations in pancake-vortex positions may be averaged, leading to an accurate "mean-field" approach where the 2D lattice in one layer sits in a substrate potential due to the attraction of the vortex stacks in all other layers. With this *substrate model* we calculate the fluctuations of individual pancake vortices, which in turn smears the substrate potential, and we solve self-consistently. The upper bound in temperature to a self-consistent solution leads to an instability line which we calculate in this paper. We then determine the melting line by comparing the free energy of the 3D PVL to the free energy of a collection of 2D liquids, using numerical results for the 2D system [10].

The evaporation at T_{BKT} of a single stack of pancake vortices occurs because each element is only logarithmically bound to the stack: A pancake vortex in a layered superconductor generates supercurrents within each layer, resulting in a pairwise interaction energy [13],

 0031-9007/00/84(12)/2698(4)$15.00

$$V_n(\mathbf{R}) = \frac{\Phi_0^2 d^2}{4\pi\lambda^2}\int \frac{d^2K dk_z}{(2\pi)^3}\,\frac{(K^2 + k_z^2)e^{i(k_z nd+\mathbf{K}\cdot\mathbf{R})}}{K^2(\lambda^{-2} + K^2 + k_z^2)}, \tag{1}$$

where n is the number of layers separating the two vortices, and $\mathbf{R}$ is the in-plane distance. The form of this interaction for different limits is well documented [1]: the in-plane repulsion is $V_0(R) = -2\varepsilon_0 d\ln(R/L)$ (where L is the system-size cutoff) and the out-of-plane attraction has the large R limit, $V_{n\neq 0}(R) = \varepsilon_0 d(d/\lambda)e^{-nd/\lambda}\ln(R/L)$. This implies that the energy to pull a single pancake vortex (of core size ξ) from a straight stack is $2\varepsilon_0 d\ln(R/\xi)$ when $R \gg \lambda$ and the entropy will unbind the pancake vortices above T_{BKT} [11].

This stack evaporation is easily reproduced within a self-consistent substrate model [14]. Here, each pancake vortex is subject to a quadratic potential, but with a strength chosen to match the thermal average ($\langle\cdots\rangle$) of the curvature in the real potential [15], $V_s(\mathbf{u}_0) = \frac{1}{2}\alpha_s u_0^2$, where $\mathbf{u}_n$ is the nth pancake vortex displacement, and $\alpha_s = \sum_{n\neq 0}\langle\partial^2_{u_0^x} V_n(\mathbf{u}_n - \mathbf{u}_0)\rangle$. Given the long range of the interactions, we can ignore correlations in the pancake vortex fluctuations and use the identity for Gaussian fluctuations that $\langle\exp[-i\mathbf{K}\cdot(\mathbf{u}_n - \mathbf{u}_0)]\rangle = \exp(-K^2\langle u^2\rangle/2)$, to give

$$\alpha_s(\langle u^2\rangle) = -\sum_{n\neq 0}\int\frac{d^2K}{(2\pi)^2}K_x^2 V_n(K)\exp\left[-\frac{K^2\langle u^2\rangle}{2}\right], \tag{2}$$

where $V_n(K) = \int d^2R e^{-i\mathbf{K}\cdot\mathbf{R}}V_n(R)$. The equipartition theorem for a harmonic potential, $\langle u^2\rangle = 2T/\alpha_s$, allows us to solve Eq. (2) self-consistently: for large displacements $\langle u^2\rangle \gg \lambda^2$, the limiting form is $\alpha_s = \varepsilon_0 d/(\langle u^2\rangle + 2\lambda^2)$, which has the solution $\langle u^2\rangle = 2\lambda^2/[1 - (2T/\varepsilon_0 d)]$, diverging at the evaporation temperature $T_{\mathrm{BKT}} = \varepsilon_0 d/2$.

We now extend this self-consistent analysis to the full 3D system at finite fields. We consider the full 2D fluctuations of the crystal in each layer, sitting on a substrate due to the stacked vortex crystals in the other layers. Before deriving this in detail, we give a quick-and-dirty derivation of evaporation at small fields. Close enough to T_{BKT} the instability occurs when $\lambda^2 \ll \langle u^2\rangle \ll a_0^2$, for a vortex density $n_v = B/\Phi_0 = (2/\sqrt{3})a_0^{-2}$. In this limit the substrate potential picks up a negative background contribution (see below), $\alpha_s \approx \varepsilon_0 d(-2\pi n_v + 1/(\langle u^2\rangle + 2\lambda^2))$. Inserting this to the equipartition result gives the quadratic equation in $\langle u^2\rangle$, $\langle u^2\rangle = (2T/\varepsilon_0 d)[2\lambda^2 + \langle u^2\rangle + 2\pi n_v\langle u^2\rangle^2]$, which only has solutions below a temperature given by $(1 - T_{\mathrm{BKT}}/T)^2 - 16\pi n_v\lambda^2 = 0$, and the instability line approaches the zero-field transition in the form

$$B_u \sim B_\lambda(1 - T/T_{\mathrm{BKT}})^2, \qquad T \to T_{\mathrm{BKT}}. \tag{3}$$

Note also that this instability occurs when the fluctuations reach the condition $\langle u^2\rangle \sim a_0\lambda$. This contrasts with the often used Lindemann criterion for melting at $\langle u^2\rangle = c_L^2 a_0^2$ (see e.g., [6]) and corresponds to a field dependent Lindemann number $c_L \sim (B/B_\lambda)^{1/4}$ (see [9] where a field-dependent c_L was also found).

A precise treatment that can be used at all fields must include the elastic distortions of the lattice within each layer. Within the self-consistent harmonic approximation (SCHA) plus substrate model the average energy cost for these distortions is given by a quadratic form, integrated over all 2D modes in the Brillouin zone, $H^{\mathrm{h}}[\mathbf{u}^0] = (1/8\pi^2)\int_{\mathrm{BZ}} d^2K u_i^0(\mathbf{K})\Phi^{ij}(\mathbf{K})u_j^0(-\mathbf{K})$ where

$$\Phi^{ij}(\mathbf{K}) = n_v\sum_{\mathbf{R}_\mu}\left[(1 - e^{i\mathbf{K}\cdot\mathbf{R}_\mu})\langle\partial_i\partial_j V_0\rangle + \sum_{n\neq 0}\langle\partial_i\partial_j V_n\rangle\right] = \varepsilon_0 d n_v^2\sum_{\mathbf{Q}_\mu}\left[f_{ij}(\mathbf{Q}_\mu + \mathbf{K}) - f_{ij}(\mathbf{Q}_\mu) + \delta_{ij}\frac{2\pi e^{-\frac{Q_\mu^2\langle u^2\rangle}{2}}}{1 + \lambda^2 Q_\mu^2}\right], \tag{4}$$

with $\mathbf{R}_\mu$ and $\mathbf{Q}_\mu$ the real and reciprocal lattice vectors and $f_{ij}(\mathbf{Q}) = Q_i Q_j(4\pi/Q^2)\exp[-Q^2\langle u^2\rangle/2]$. The first two terms in (4) are the 2D elasticity and the last is the contribution from the substrate. Again, we have ignored correlations in displacements $\langle u_i^m(\mathbf{R}_\mu)u_j^n(\mathbf{R}_\nu)\rangle = \delta_{\mu\nu}\times\delta_{mn}\delta_{ij}\langle u^2\rangle/2$ in the last line. Note that the $\mathbf{Q}_\mu = 0$ substrate term is canceled by the $\mathbf{Q}_\mu = 0$ part of the second 2D-elastic term. This is a reflection of the long range divergences in the 2D system with log (Coulomb) interactions, which do not exist for the 3D system of stacks where the circulation currents are screened beyond λ.

The elastic matrix decomposes to transverse $(\delta_{ij} - \hat{K}_i\hat{K}_j)\Phi^{ij}(\mathbf{K}) = c_{66}(\mathbf{K})K^2 + n_v\alpha_s$ and longitudinal $\hat{K}_i\hat{K}_j\Phi^{ij}(\mathbf{K}) = c_{11}(\mathbf{K})K^2 + n_v\alpha_s$ projections, where c_{66} and c_{11} are the dispersive shear and compression moduli, and α_s is the substrate strength, $\alpha_s = 2\pi\varepsilon_0 d n_v\sum_{\mathbf{Q}_\mu\neq 0}\exp[-Q_\mu^2\langle u^2\rangle/2]/(1 + \lambda^2 Q_\mu^2)$. The $\langle u^2\rangle \to 0$ limit of c_{66} and c_{11} recovers the usual form for the elasticity of a 2D vortex lattice [16], with a shear modulus $c_{66}^0 = n_v\varepsilon_0 d/4$ and a diverging compression modulus $c_{11}^0(K) = 4\pi\varepsilon_0 d n_v^2/K^2$ at small K. A finite $\langle u^2\rangle$ softens these moduli, although the diverging compression modulus remains [15]. To solve self-consistently for $\langle u^2\rangle$ we use the equipartition result

$$\begin{aligned}\langle u^2\rangle &= T\int_{\mathrm{BZ}}\frac{d^2K}{(2\pi)^2}[\Phi^{-1}]^{ii}(\langle u^2\rangle, \mathbf{K})\\ &\approx \frac{T}{4\pi c_{66}}\ln\left(1 + \frac{c_{66}K_{\mathrm{BZ}}^2}{n_v\alpha_s}\right) + \frac{T}{4\pi c_{11}(K_{\mathrm{BZ}}) + \alpha_s},\end{aligned} \tag{5}$$

where in the last line we have used a nondispersive c_{66} and a dispersive c_{11}, and have taken a circular Brillouin zone with $K_{\mathrm{BZ}} \approx \sqrt{4\pi}/a_0$. Note how the substrate potential cuts off the log divergence for the 2D shear fluctuations.

The self-consistent Eqs. (4) and (5) determine $\langle u^2\rangle$. Above a temperature T_u there are no solutions, giving an upper bound to the melting transition. However, in [15] it was shown that the SCHA underestimates the degree

of anharmonic thermal softening of a 2D lattice. Using a diagrammatic perturbation theory about the harmonic approximation, one finds that the SCHA includes only simple diagrams with even vertices; odd terms in the anharmonicity are neglected. In [15] a new technique that includes cubic anharmonicities, the two-vertex SCHA, is shown to give results that compare well to numerical simulations. In particular, a thermal instability of the lattice occurs much sooner than predicted by the simple SCHA. In Fig. 1 we show the instability line of the PVL in the B-T phase diagram using the two-vertex SCHA. The line interpolates between at small fields and T_m^{2D} at high fields. Also shown is the significant thermal softening of both c_{66} and α_s at $B = B_\lambda$ with the resulting anharmonic contributions (beyond linear in T) for $\langle u^2 \rangle$.

The above instability line marks only the upper temperature limit of the solid phase. A true first-order transition occurs when the free energies of two phases cross. For melting transitions it is often difficult to accurately determine the free energy of the liquid. We can make progress for PVL melting, as the liquid state behaves to a good approximation as uncoupled 2D liquids in each layer. The free energy of a 2D liquid with log interactions can be extracted from numerical simulations [10]. A crucial ingredient is that the free energy is known exactly [17] at one special temperature $T = \varepsilon_0 d$. For the solid we calculate the free energy of a 2D crystal on a self-consistent substrate. We must be careful to take the same normalization in both phases: as in [17] we normalize with respect to the ideal gas of N pancakes, $Z(H = 0) = 1$, and define the partition function,

$$Z = \frac{1}{N!} \int \prod_i \left(\frac{n_v}{e} \right) d^2 R_i e^{-H[\mathbf{R}_i]/T}, \tag{6}$$

fixing the free energy, measured from the ideal gas, as $F = -T \ln Z$. We write $H = H_{2D} + H_s$ where $H_{2D} = (N/2)[\sum_{\mathbf{R}_\mu \neq 0} V_0(R_\mu) - n_v \int d^2 R V_0(R)]$ and $H_s = (N/2)[\sum_{\mathbf{R}_\mu, n \neq 0} V_n(R_\mu) + n_v \int d^2 R V_0(R)]$ are the 2D interaction term and substrate energy, respectively [18].

In the solid, the free energy of harmonic fluctuations is straightforward to calculate. The right-hand side of the inequality $F \leq F^h + \langle H - H^h \rangle_h$ is minimized by the SCHA (see [15]) where H^h is defined by (4). The harmonic free energy of 2D fluctuations is

$$F^h = -\frac{NT}{2n_v} \int_{BZ} \frac{d^2K}{(2\pi)^2} \left[\ln\left(\frac{\pi T n_v^2}{e(c_{66}K^2 + n_v \alpha_s)} \right) + \ln\left(\frac{\pi T n_v^2}{e(c_{11}K^2 + n_v \alpha_s)} \right) \right]. \tag{7}$$

The correction part of the variational free energy has contributions from H_{2D} and H_s. Ignoring the small anharmonic part of the 2D energy, the difference $\langle H_{2D} - H_{2D}^h \rangle_h$ is just the ground state energy (which is not included in H_{2D}^h). In [17] the energy for a 2D lattice of log-interacting particles is found to be $E_{2D}^0 = 0.749 N \varepsilon_0 d$. The substrate energy correction, $E_s = \langle H_s - H_s^h \rangle_h$, is

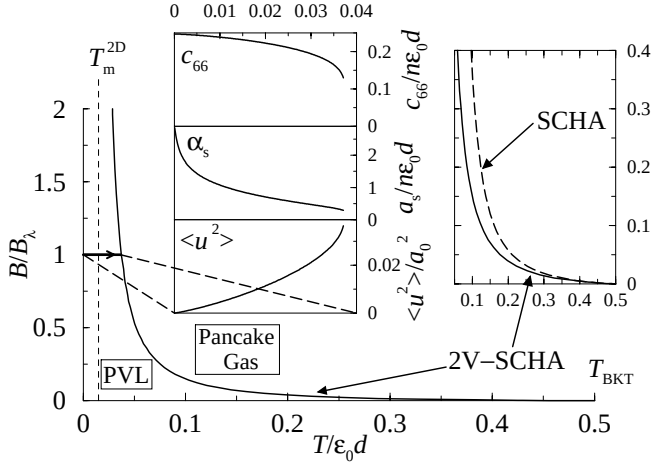

FIG. 1. The instability line for the PVL in the B-T plane calculated with the two-vertex SCHA. The line goes asymptotically to the 2D melting temperature at high fields, and ends at T_{BKT} at zero field. Left inset: shear modulus c_{66}, substrate strength α_s, and pancake fluctuation width $\langle u^2 \rangle$ versus temperature at $B = B_\lambda$. Right inset: low-field zoom of the instability line showing the result (dashed) of the simple SCHA scheme for comparison: the SCHA overestimates the stability of the lattice at high fields. We do not include here the intrinsic temperature dependence in real superconductors of the penetration depth and the energy scale ε_0 (but see Fig. 2).

$$E_s = -N \left[2\pi n_v \varepsilon_0 d \sum_{\mathbf{Q}_\mu \neq 0} \frac{e^{-Q_\mu^2 \langle u^2 \rangle/2}}{Q_\mu^2 (1 + \lambda^2 Q_\mu^2)} + \frac{1}{2} \alpha_s \langle u^2 \rangle \right], \tag{8}$$

and the sum $F^h + E_{2D}^0 + E_s$ is the variational free energy.

In the liquid phase, $\langle H_s \rangle$ is very small and we should find the free energy of a 2D liquid. The internal energy $U(\Gamma)$ (with $\Gamma = 2\varepsilon_0 d/T$) is found from simulations [10],

$$U(\Gamma) = (-0.751 + 0.880\Gamma^{-0.74} - 0.209\Gamma^{-1.7}) N \varepsilon_0 d\,. \tag{9}$$

From the relation $F = U + T\partial_T F$, the excess free energy can be written as $\Gamma F_{liq}(\Gamma) = \Gamma_0 F_{liq}(\Gamma_0) + \int_{\Gamma_0}^{\Gamma} U(\Gamma') d\Gamma'$. We know the value at $\Gamma_0 = 2$, where $F_{liq}(2) = 0.081 \varepsilon_0 dN$ [17], so we can integrate (9) to give (with $t = T/\varepsilon_0 d$),

$$F_{liq} = (-0.751 - 1.287t + 2.027t^{0.74} + 0.092t^{1.7}) \times N \varepsilon_0 d\,. \tag{10}$$

Using these results we can plot the free energy of both phases and see where they cross; a typical example at $B = B_\lambda$ is shown in the inset of Fig. 2. Calculating the crossing point numerically at different fields, we find a melting line (see Fig. 2) just below the stability limit of the lattice that approaches zero field at $T \approx 0.47 \varepsilon_0 d$.

The jump in slope $S = -\partial_T F$ gives a latent heat $T\Delta S = \Delta U$. In Fig. 2 we plot the entropy jump per pancake vortex as a function of the transition temperature. At high fields (small T) it approaches the value $\Delta s_v \approx 0.4 k_B T_{BKT}$, consistent with 2D simulations [10] and simple estimates [19]. At low fields ($T \sim 0.5 \varepsilon_0 d$)

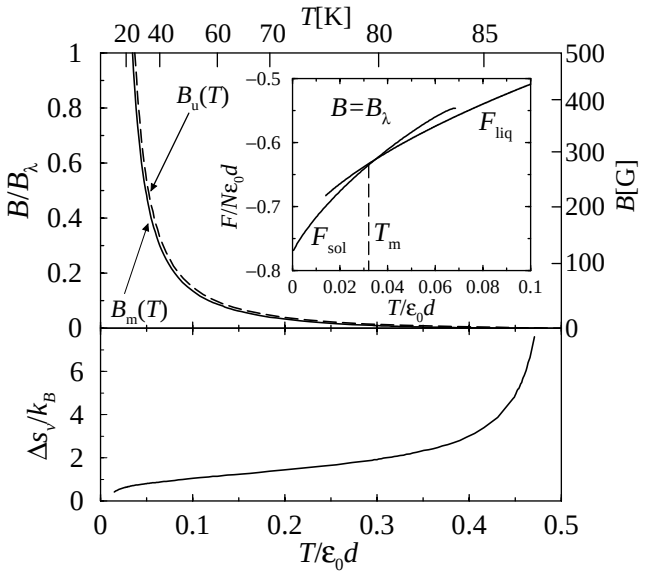

FIG. 2. The full line in the upper graph shows the melting line $B_m(T)$ of the pancake vortex lattice as calculated by comparing the free energies of the solid and liquid phases. The dashed line is the stability limit $B_u(T)$ of the PVL as shown in Fig. 1. The inset shows the free energy comparison at $B = B_\lambda$. The lower graph gives the entropy jump per pancake vortex Δs_v. Also shown are the real scales of T and B assuming $\lambda(T) = \lambda(0)/[1 - (T/T_{c0})^2]^{1/2}$, with $\lambda(0) \approx 2000$ Å, $d \approx 15$ Å, and $T_{c0} \approx 100$ K. The low-field reentrant melting line, not shown here, will cut $B_m(T)$ below $10^{-2}B_\lambda$.

the latent heat appears to weakly diverge as $T \to T_{\mathrm{BKT}}$. We understand this as the energy of the liquid is roughly constant, $U(T \approx T_{\mathrm{BKT}}) \approx -0.219N\varepsilon_0 d$, while the energy of the solid is dominated by the substrate term, $E_s \sim N\varepsilon_0 d \ln(\lambda/a_0)$ so that the latent heat is $\Delta U \sim -E_s$. This gives an entropy jump per vortex pancake $\Delta s_v = \Delta U/NT \sim k_B \ln(B_\lambda/B)$. This is of the same form as the entropy difference between an ideal gas, $\Delta s_v^{\mathrm{gas}} \approx k_B \ln(a_0^2/\xi^2)$ and the (reduced phase-space) solid $\Delta s_v^{\mathrm{sol}} \approx k_B \ln(\langle u^2\rangle/\xi^2)$ when $\langle u^2\rangle \sim a_0\lambda$ (as found above for the low-field instability). We do not include here the T dependence of λ in real systems that gives extra terms in the latent heat [19].

Previously, melting of the magnetically coupled PVL has been analyzed numerically [8] and via density functional theory (DFT) of the liquid phase [20]. The early simulations in [8] find evidence of melting at $T \approx 0.09\varepsilon_0 d$ when $B/B_\lambda \approx 0.2$ (close to our melting line). The DFT gives the stability limit of the liquid and provides results consistent with ours at fields above $0.5B_\lambda$. At lower fields the DFT gives a liquid instability above our melting line, calling for further study. Note that the DFT, numerical simulations, and our calculation do not include the thermal proliferation of bound vortex-antivortex pairs, which will effect the results close to T_{BKT}.

To compare to real superconductors our units of field B_λ and of temperature $\varepsilon_0 d$ must be scaled due to the intrinsic variation in $\lambda(T)$ (diverging at a temperature T_c^0). Doing this, we find that our melting curve of Fig. 2 lies below experimental melting lines [2,21] for reasonable choices of $\lambda(T)$; this is because the Josephson coupling, neglected in this paper, becomes important as T_c^0 is approached [6] and stiffens the vortex lattice. Our results may be recovered in experiments by suppressing the Josephson coupling with a strong in-plane magnetic field.

We thank Misha Feigelman and Lev Bulaevskii for useful discussions. Work in Zürich was financially supported by the Swiss National Foundation and in Argonne by the NSF Office of the Science and Technology Center under Contract No. DMR-91-20000 and the U.S. DOE, BES-Materials Sciences, under Contract No. W-31-109-ENG-38.

*Present address: Theory of Condensed Matter Group, Cavendish Laboratory, Cambridge, CB3 0HE, U.K.

[1] G. Blatter *et al.*, Rev. Mod. Phys. **66**, 1125 (1994).
[2] E. Zeldov *et al.*, Nature (London) **375**, 373 (1995).
[3] A. Schilling *et al.*, Nature (London) **382**, 791 (1996).
[4] D. T. Fuchs *et al.*, Phys. Rev. Lett. **80**, 4971 (1998).
[5] A. Houghton *et al.*, Phys. Rev. B **42**, 906 (1990).
[6] G. Blatter *et al.*, Phys. Rev. B **54**, 72 (1996).
[7] R. Šášik and D. Stroud, Phys. Rev. Lett. **75**, 2582 (1995); J. Hu and A. MacDonald, Phys. Rev. B **56**, 2788 (1997); H. Nordborg and G. Blatter, Phys. Rev. Lett. **79**, 1925 (1997); A. E. Koshelev, Phys. Rev. B **56**, 11 201 (1997); X. Hu *et al.*, Phys. Rev. Lett. **79**, 3498 (1997); A. K. Nguyen and A. Sudbo, Phys. Rev. B **58**, 2802 (1998); P. Olsson and S. Teitel, Phys. Rev. Lett. **82**, 2183 (1999).
[8] D. Reefman and H. B. Brom, Physica (Amsterdam) **183C**, 212 (1991).
[9] S. Ryu *et al.*, Phys. Rev. Lett. **68**, 710 (1992).
[10] J. M. Caillol *et al.*, J. Stat. Phys. **28**, 325 (1982).
[11] J. R. Clem, Phys. Rev. B **43**, 7837 (1991); L. N. Bulaevskii *et al.*, Phys. Rev. B **43**, 3728 (1991).
[12] V. L. Berezinskii, Sov. Phys. JETP **32**, 493 (1971); J. M. Kosterlitz and D. J. Thouless, J. Phys. C **6**, 1181 (1973).
[13] S. N. Artemenko and A. N. Kruglov, Phys. Lett. A **143**, 485 (1990); M. V. Feigelman, V. B. Geshkenbein, and A. I. Larkin, Physica (Amsterdam) **167C**, 177 (1990); A. Buzdin and D. Feinberg, J. Phys. (France) **51**, 1971 (1990).
[14] M. J. W. Dodgson, V. B. Geshkenbein, and G. Blatter, Physica (Amsterdam) B (to be published).
[15] M. J. W. Dodgson *et al.* (to be published).
[16] E. H. Brandt, J. Low Temp. Phys. **26**, 735 (1977).
[17] A. Alastuey and B. Jancovici, J. Phys. (Paris) **42**, 1 (1981).
[18] Note that we add and subtract the background energy from a continuous opposite charge, as the diverging energy of the 2D log system must cancel for 3D stacks.
[19] M. J. W. Dodgson *et al.*, Phys. Rev. Lett. **80**, 837 (1998).
[20] S. Sengupta *et al.*, Phys. Rev. Lett. **67**, 3444 (1991); G. I. Menon *et al.*, Phys. Rev. B **54**, 16 192 (1996); P. S. Cornaglia and C. A. Balseiro, cond-mat/9904183.
[21] S. L. Lee *et al.*, Phys. Rev. B **55**, 5666 (1997).